

Synthesis and Characterization of Hydroxyapatite based on Green Mussel Shells (*Perna viridis*) with Calcination Temperature Variation Using the Precipitation Method

Mona Sari¹ and Yusril Yusuf^{2*}

^{1,2}Department of Physics, Universitas Gadjah Mada, Yogyakarta 55281, Indonesia.

Received 7 November 2017; Revised 3 December 2017; Accepted 25 January 2018

ABSTRACT

Hydroxyapatite (HA) from green mussel shells (*Perna viridis*) has been successfully synthesized with a variation of calcination temperature using the precipitation method. Green mussel shells were calcined in a furnace at temperatures of 650°C, 750°C, 850°C and 950°C for 2 h to obtain calcium oxide. AAS results show that the levels of Ca for calcination at temperatures of 650°C, 750°C, 850°C, and 950°C are 30.4333%, 34.3030%, 37.1080% and 49.5757%, respectively. X-Ray diffractometer results show that the crystallization of calcium oxide with calcination at 950°C is high because of its large crystallite size and small microstrain. SEM results reveal some relief lines on the particle surfaces, products of the high temperatures (850°C and 950°C) during calcination. TGA analysis indicates that green mussel shells calcined at 950°C experience a significant weight loss of 22.386%. XRD analysis shows that the HA with a stirring time of 60 min exhibits high crystallinity, with a large crystallite size of (82.50 ± 5.3) nm and the smallest microstrain value (0.0061). DTA/TGA analysis reveals that HA with a stirring time of 60 min undergoes faster weight loss in the temperature of 426.33°C, with a weight loss of 0.834%. The FTIR spectra show that HA with a stirring time of 60 min shows the functional group of CO_3^{2-} only at 875.62 cm^{-1} . This indicates that the samples' CO_3^{2-} is low. SEM results demonstrate that HA with a stirring time of 60 min has a small agglomerate shape and thick particles structure. EDX analysis reveals that HA with a stirring time of 60 min exhibits a Ca/P molar ratio of 1.67, the Ca/P molar ratio of HA.

Keywords: Calcination Temperature, Green Mussel Shells, Hydroxyapatite, Precipitation.

1. INTRODUCTION

Osteoporosis is one of the leading causes of bone damage. While osteoporosis is associated most commonly with older populations, bone loss can affect anyone, including those at a young age. A recent study by the International Osteoporosis Foundation (IOF) revealed that one in four women in Indonesia between the ages of 50 and 80 years are at risk of osteoporosis, a risk rate four times higher than that of men in Indonesia. The results of a white paper study conducted by the Association of Osteoporosis Indonesia in 2007 reported that the proportion of osteoporosis patients aged over 50 years was 32.3% among women and 28.8% in men [1]. To further this risk, the rate of accidents (both minor accidents and serious accidents that result in bone damage) per year has increased.

*Corresponding Author: yusril@ugm.ac.id

Typically, treatments for bone damage involve using heavy metals to replace damaged bones. However, this presents a problem as the metals have low biocompatibility levels in the body, which can cause illness or bruising in the tissue around the metal. To combat this, the metals are coated with a biocompatible material before implantation. Previously, this coating was made from materials already existing in the body: constituents of bone tissue such as apatite compounds.

Now, however, an artificial bone compound similar to the original bone constituent has become available: hydroxyapatite [2].

Hydroxyapatite— $\text{Ca}_{10}(\text{PO}_4)_6(\text{OH})_2$, or more simply, HA—is a major component of human bones and teeth [3]. It is commonly used in orthopedic, dental and maxillofacial applications [4,5,6]. HA has a stable potassium phosphate crystal phase, a hexagonal structure, lattice parameters of $a = 9.433\text{\AA}$ $c = 6.875\text{\AA}$ and a variable Ca/P mol ratio is 1.67 [7,8]. The advantages of hydroxyapatite are porous, bioactive, non-corrosive and wear-resistant. HA has a weight of 69% of the weight of pure bone and is the most stable compound in body fluids and dry air up to the temperature of 1200°C [9].

A variety of synthesis techniques of hydroxyapatite have been developed such as sol-gel procedure [10], precipitation from aqueous solution [11], and hydrothermal [12,13,14] and solid-state reactions [15]. In this study, the precipitation method is used to synthesize HA. Precipitation methods were selected per several considerations. Many HA, for example, are synthesized without the use of organic solvents (at relatively low cost), which is a simple process with a large output (87%), making the method suitable for large-scale (i.e., industrial) production. This requires inexpensive reagents and Ca/P products with the appropriate phase compositions. Although this process depends on variables such as pH, aging and temperature, it is more effective and inexpensive than sol-gel. HA made by chemical synthesis is called synthetic HA. Synthetic HA can be obtained not only through the reaction of synthetic compounds but also with natural compounds. HA can be synthesized from materials that are high in calcium, such as cow bones, fish bones, cuttlefish, eggshells and mussel shells [16].

In this study, waste mussel shells from Indonesia are used as the natural compound for chemical synthesis. Mussel shell production in Indonesia has been on the rise since 2002 [17]. Waste mussel shells are high in calcium carbonate at 95% to 99% [18], so they can be used as a source of calcium for HA synthesis. Energy Dispersive X-Ray Fluorescence (EDXRF) analyses show that the minor mineral composition in green mussel shells are Ca 99.5%, Sc 0.24% and Sr 0.47% [19].

The HA in this study is synthesized via the precipitation method using CaCO_3 from green mussel shells and calcination temperatures of 650°C , 750°C , 850°C and 950°C to obtain the best calcium oxide. Stirring times of 60 min are applied using the best characterization results from the calcium oxide at 70°C . To assess the feasibility of the material's use as an implant material (especially as a metal coating), the effect of the variation of calcination temperatures on the HA's characteristics from the green mussel shells is observed, including its effect on crystallinity, Ca/P ratio, thermal and stability properties and the functional groups of OH^- , PO_4^{3-} and CO_3^{2-} in the HA samples.

2. MATERIALS AND METHODS

2.1 Preparation of Calcium Oxide

The waste green mussel shells (*Perna viridis*) were cleaned in boiling water for 30 min and then washed using distilled water to remove attached materials such as shell meat and algae. They were dried in a furnace at a temperature of 100°C . To reduce the shells to a smaller particle size,

a ball mill was used. The powdered green mussel shells were heated at temperatures of 650°C, 750°C, 850°C and 950°C for 2 h to obtain the calcium oxide powder.

2.2 Synthesis of Hydroxyapatite

An amount of 2 g of calcium oxide was mixed with 50 ml of distilled water. Then, an $(\text{NH}_4)_2 \text{HPO}_4$ solution (2.8285 g in 50 ml distilled water) was slowly added dropwise at a rate of 1 ml/min to the calcium oxide powder. The liquid mixture was stirred at a velocity of 300 rpm for 60 min at a temperature of 70°C. The pH of the mixture was controlled above 9 by adding ammonium hydroxide (NH_4OH , 25 %) 3M. The mixture was then stirred by a magnetic stirrer for 50 min at 70°C. The solution was subjected to an aging treatment for 24 hour and washed using distilled water. The solution was filtered to obtain the precipitate of HA. The precipitate of HA was dried at a temperature of 100°C for 2 hour. Finally, the HA was calcined at 950°C for 3 hour using the furnace to obtain the pure HA.

2.3 Characterization

In the preparation stage, the green mussel shell sample was characterized using an atomic absorption spectrophotometer (AAS) to determine the level of Ca in the green mussel shells. The calcium oxide was characterized using an x-ray diffractometer (XRD) to determine the crystallite size and microstrain. The calcium oxide was characterized using Differential Thermal Analysis/Thermogravimetric Analysis (DTA/TGA) to analyze its thermal and stability properties. Fourier Transform Infrared Spectroscopy (FTIR) was used to determine the functional groups of the calcium oxide, and Scanning Electron Microscopy (SEM) was used to determine the morphology of the calcium oxide [20].

During synthesis, the HA samples were characterized using XRD to determine the HA's crystal structure, and DTA/TGA was conducted to analyze the samples' thermal and stability properties. FTIR was used to identify the functional groups of OH^- , PO_4^{3-} and CO_3^{2-} in the HA samples. SEM was used to determine the morphology of the HA samples [20].

3. RESULTS AND DISCUSSION

3.1 Calcination

The green mussel shells had to be calcined before they could be used as calcium precursors (Ca). Calcination was done to trigger the decomposition reaction of calcium carbonate (CaCO_3) to calcium oxide (CaO). In this condition, all organic components of the green mussel shells were burned to CaO and H_2O . The reaction for this calcination process was as follows:



The enthalpy change for the decomposition reaction of CaCO_3 was 177.7 kJ/mol [21]. This means that the enthalpy change for the decomposition reaction of CaCO_3 was positive, so the occurring reaction was an endothermic one [21]. Sample calcination was performed at 650°C, 750°C, 850°C and 950°C because the decomposition reaction of CaCO_3 to CaO was possible at a minimum of 750°C [22]. Per calculations using the enthalpy concept, the parameter for increasing the temperature was 1426°C, meaning the calcination temperature variations could ideally be carried out at ~1400°C. Providing heat greatly helped the optimization of the decomposition reaction. When the CaCO_3 compounds received the heat, the atoms moved faster; this movement broke the chemical bonds of CaCO_3 into CaO and CO_2 . Increasing the calcination temperature inclined the breaking of the chemical bonds CaCO_3 into CaO to occur faster [23].

The AAS analysis showed that the Ca levels at the calcination temperatures of 650°C, 750°C, 850°C and 950°C were 30.4333%, 34.3030%, 37.1080% and 49.5757%, respectively. This demonstrates that increasing the calcination temperature causes the level of Ca to increase. According to the XRD analysis results, the samples calcined at 650°C, 750°C, 850°C and 950°C exhibited diffraction angles (2θ) of 29.08°, 29.12°, 28.82° and 29.02°, respectively. The obtained crystallite size and microstrain calculations for the CaO samples are shown in Table 1.

Table 1 Crystallite size and microstrain for calcium oxide samples

Samples	Crystallite Size (nm)	Microstrain
Calcination at 650°C	149.35 ± 6.9	0.00370
Calcination at 750°C	182.36 ± 7.5	0.00301
Calcination at 850°C	164.61 ± 8.1	0.00340
Calcination at 950°C	184.80 ± 7.9	0.00302

As shown in Table 1, increasing the calcination temperature caused the crystallite size to grow. However, crystallite size decreased at a calcination temperature of 850°C. This result was later confirmed in the FTIR spectra results and the results of the DTA/TGA that assessed thermal properties and stability. Calcined CaO at a temperature of 950°C obtained a large crystallite size so that the crystallinity was also high and the amorphous phase level decreased. The calcined CaO at 950°C obtained a small microstrain compared to the samples calcined at other temperatures. Microstrain is a form of crystal imperfection that appears as a distortion or dislocation. A small microstrain value indicates a small amount of defect in the crystal [24].

FTIR spectra analysis was performed on the CaO to identify whether the functional groups of C-O, OH⁻ and CaO formed. As shown in Fig.1, the non-calcined green mussel shells did not show the stretching mode of OH⁻ or the functional group of CaO. The green mussel shells calcined at 650°C and 750°C indicated stretching modes of OH⁻ at 3629.77 cm⁻¹, while the green mussel shells calcined at 850°C and 950°C indicated stretching modes of OH⁻ at 3641.34 cm⁻¹. All five samples of CaO exhibited C-O functional groups of calcium carbonate in the green mussel shells. The functional bands of calcium carbonate indicated closeness to the commercial calcium carbonate functional group at 1400 cm⁻¹, 877 cm⁻¹ and 700 cm⁻¹ [25].

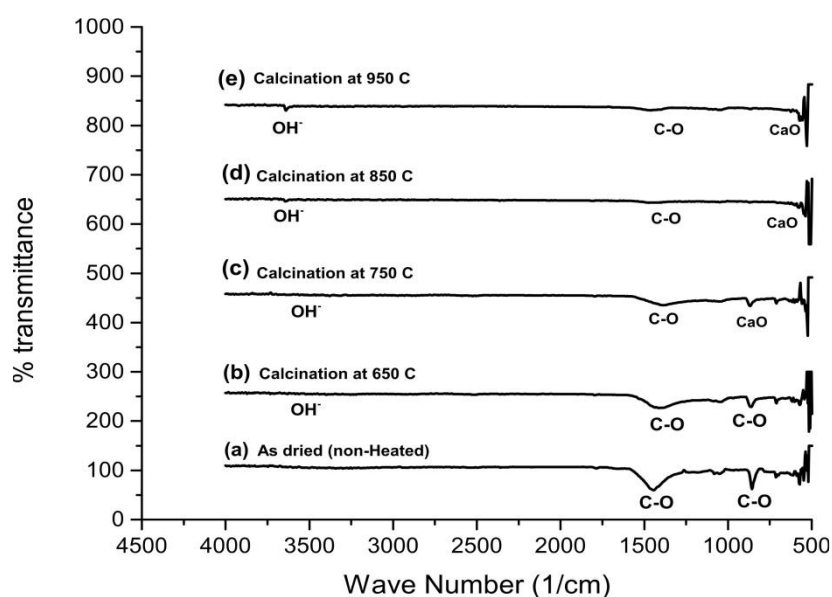


Figure 1. FTIR spectra of samples: non-calcination (a), calcination at 650°C (b), 750°C (c), 850°C (d) and 950°C (e).

Formation of the CaO functional group began when CaO was calcined starting at 750°C at 867.90 cm^{-1} . The CaO functional groups increased as the temperature of calcination was raised. This result can be seen in the CaO functional groups at the calcination temperatures of 850°C and 950°C at 871.76 cm^{-1} ; even the CaO calcined at 950°C showed CaO bond formation at 667.32 cm^{-1} . This demonstrates that while formation of the OH⁻ functional group started when the green mussel shells began to calcine at 650°C, formation of the CaO functional group started when calcination of the green mussel shells began at 750°C.

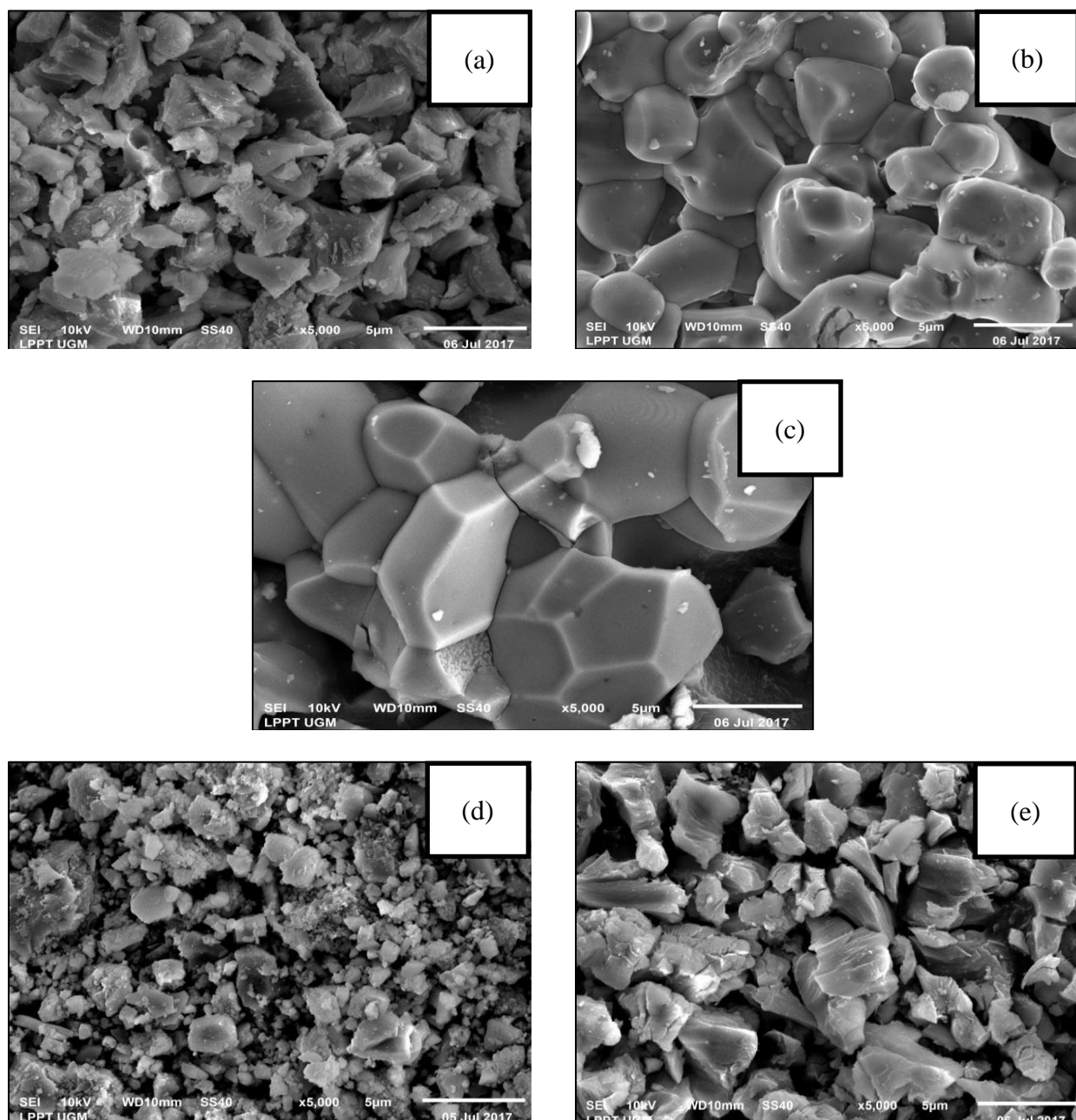


Figure 2. Results of SEM characterization for five samples: green mussel shells (a), calcination temperature of 650°C (b), 750°C (c), 850°C (d) and 950°C (e).

SEM characterization was performed to determine the morphology of the green mussel shells and the calcium oxide from the shells. Images were taken using 5000x magnification. As shown in Figure 2(a), the green mussel shells had a large particle shape with heterogeneous particle distribution. The morphology of the shells resembled cavities. The green mussel shells calcined

at 650°C had a plate-like shape with large, coarse particles. In Figure 2(c), the green mussel shells calcined at 750°C are shown to have a large and irregular particle shape. In Figure 2(d) and 2(e), some relief lines are visible on the surface of the particles, the product of calcination at 850°C and 950°C.

The morphology of the green mussel shells differed considerably from that of the calcium oxide, indicating that the calcination process released CO₂ and created cavities. This structure of the calcined shells aided the reaction with deionized water to hydrolyze the calcium oxide to calcium hydroxide and form a solid suspension/slurry of calcium hydroxide for the preparation of HA.

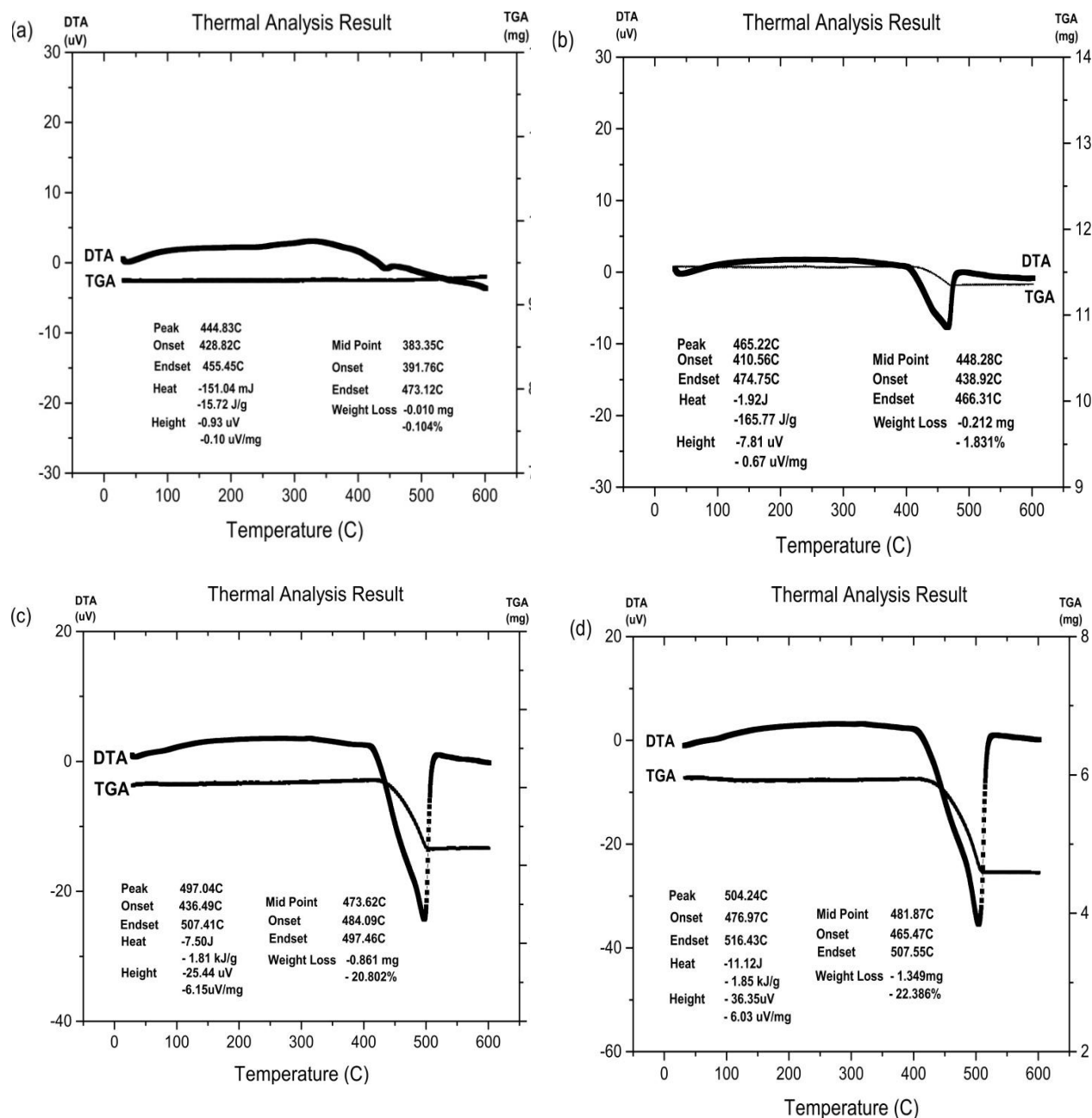


Figure 3. DTA/TGA results of calcium oxide at calcination temperatures (a) 650°C, (b) 750°C, (c) 850°C and (d) 950°C.

Per Figure 3, the green mussel shells calcined at temperatures of 650°C, 750°C, 850°C and 950°C decreased in weight at 391.76°C, 438.92°C, 484.09°C and 465.47°C, respectively, with weight loss percentages of 0.104%, 1.831%, 20.802% and 22.386%, respectively. The most significant weight loss occurred in the green mussel shells calcined at 950°C. This result indicates that large amounts of calcium carbonate content decompose into calcium oxide at the temperature of the calcination. After conducting the AAS, XRD, FTIR, DTA/TGA and SEM analyses, the calcium oxide sample calcined at 950°C was used to synthesize HA with a stirring time of 60 min.

3.2 XRD Analysis of the Hydroxyapatite

XRD characterization can be used to determine the crystal system, crystallite size, lattice parameter, crystallinity and phase of a sample. The XRD pattern for the HA from the green mussel shells is shown in Figure 4. The HA with a stirring time of 60 min peaked at 31.70° with an *hkl* index close to 211. These results agreed with data from the Joint Crystal Powder Diffraction Standard (JCPDS) No.09-0432.

Using calculations made with the Bragg equation [26], the distance between the crystal planes of the HA with a stirring time of 60 min was determined at 2.85Å. This result was close to the crystal plane of the HA at 2.88Å, making it appropriate by international standards (ISO 13779-3, ISO 13175-3) for HA implants [27].

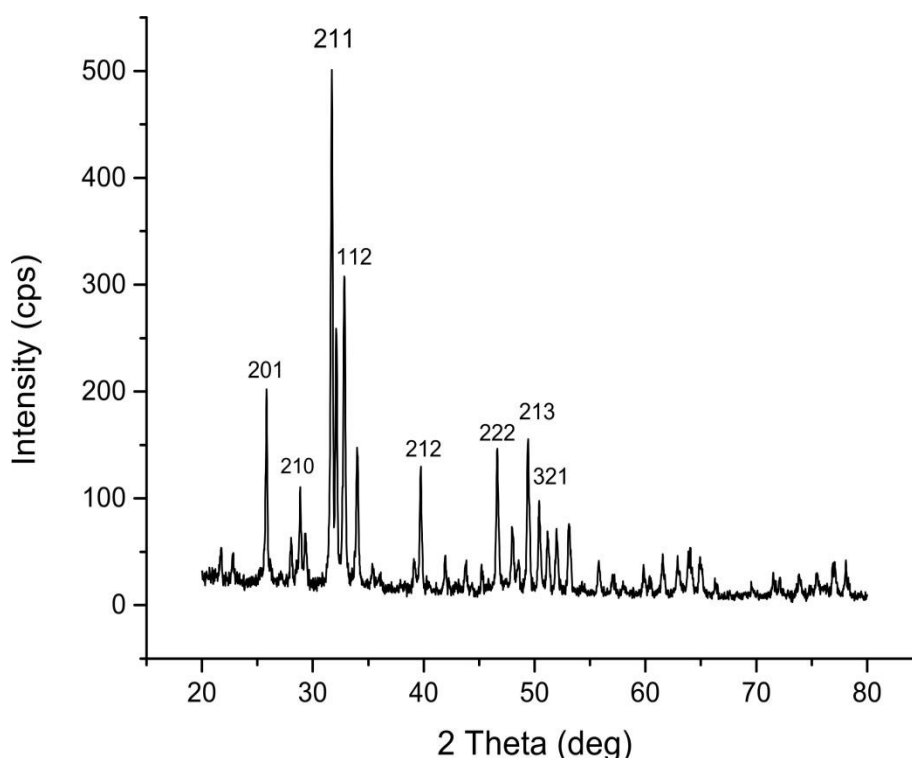


Figure 4. XRD pattern of the synthesized HA with a stirring time of 60 min.

The crystallite size, microstrain, lattice parameter and x-ray density of the synthesized HA were (82.5 ± 5.3) nm, 0.0061, 8.66Å and 10.27g/cm³, respectively. According to these data, the x-ray density value corresponded to the parameter lattice of the sample. This means that the crystallization of the HA depended on the stirring time. If the stirring time was longer than 15 min, no HA was produced.

3.3 FTIR Spectra of the HA Sample

As revealed by the FTIR spectra shown in Figure 5, the HA with a stirring time of 60 min exhibited the functional group of HA. HA with a stirring time of 60 min exhibited the stretching mode of OH⁻ at 3645.19 cm⁻¹ and 3571.90 cm⁻¹. HA with a stirring time of 60 min exhibited the bending mode of OH⁻ at 628.75 cm⁻¹ and bending modes of stretching ν (P-O) mode of PO₄³⁻ at 960.48, 1026.05 and 1087.77 cm⁻¹. HA with a stirring time of 60 min also exhibited increases in bending (P-O) PO₄³⁻ at 570.89 and 601.75 cm⁻¹. HA with a stirring time of 60 min exhibited the functional group of CO₃²⁻ only at 875.62 cm⁻¹.

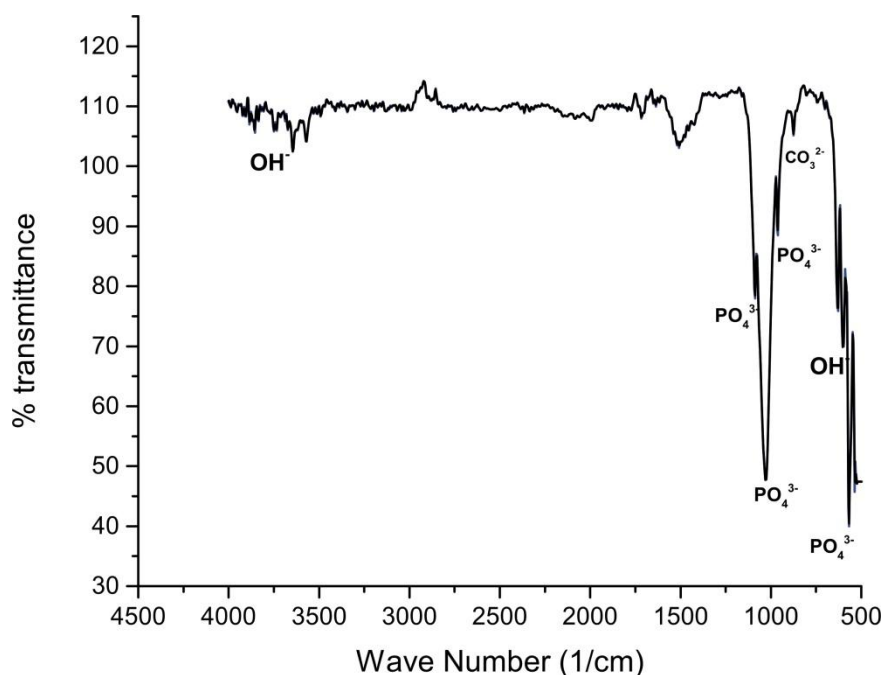


Figure 5. FTIR spectra of synthesized HA with a stirring time of 60 min.

The existence of CO₃²⁻ groups in the FTIR spectra were due to the reaction of calcium oxide with carbon dioxide in free air during synthesis. However, CO₃²⁻ groups may have existed in the raw green mussel shells before the synthesis process. Carbon dioxide came into contact with the distilled water solvent in this reaction and released CO₃²⁻ into the crystal lattice of the HA.

The carbonate entering the crystal lattice affected the Ca/P ratio and the crystal area. The carbonate ions occupied two positions in the HA's structure, replacing the OH⁻ group to form an A-type apatite carbonate (AKA) with a chemical formula (Ca₁₀(PO₄)₆CO₃) or replacing the PO₄³⁻ group to form a B-type apatite carbonate with the chemical formula of (Ca₁₀(PO₄)₃(CO₃)₃(OH)₂). The CO₃²⁻ ions caused the contraction of the lattice parameter (*a*) of the HA structure. While the main cause of the carbonate ions' release into the crystal lattice was the mixing reaction of the precursors in open air, other factors also contributed; these include the slow addition of (NH₄)₂HPO₄ (1ml/min). The existence of carbonate in the HA structure was found to reduce the HA's thermal stability, as confirmed by the DTA/TGA results. These results indicate that if the calcium carbonate content is high, the sample decreases significantly. The existence of CO₃²⁻ groups is common because they occur naturally in human bones. This makes them a natural substitution for PO₄³⁻, per the formula for molecules Ca₁₀(CO₃)_x(PO₄)_{6(2/3)x}(OH)₂, otherwise called "carbonated HA". The existence of carbonate is unavoidable if HA synthesis is conducted in the open air. Therefore, there needs to be an environmental inertization (reactor) that passes inert gas, such as nitrogen (N₂), so that the process of precursor mixing is free from outside air contamination [28].

3.4 SEM-EDX Results

The morphology of the HA with a stirring time of 60 min is shown in Fig. 6. This image was taken with a magnification of 10000x. The HA showed a small agglomerate shape and solid structure. Its morphology resembled granules with uniform grains, but it had a rough surface. The SEM results showed that the HA synthesized using the precipitation method produced a fine grain of uniform size

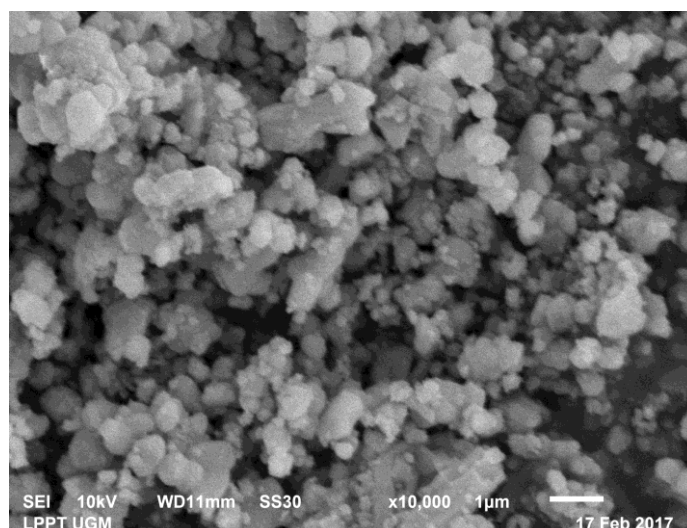


Figure 6. SEM images of synthesized HA with a stirring time of 60 min.

The EDX analysis was performed to determine the element composition contained in the HA and the ratio of Ca/P. As shown in Figure 7 and Table 2, the HA with a stirring time of 60 min also exhibited a Ca/P molar ratio of 1.67.

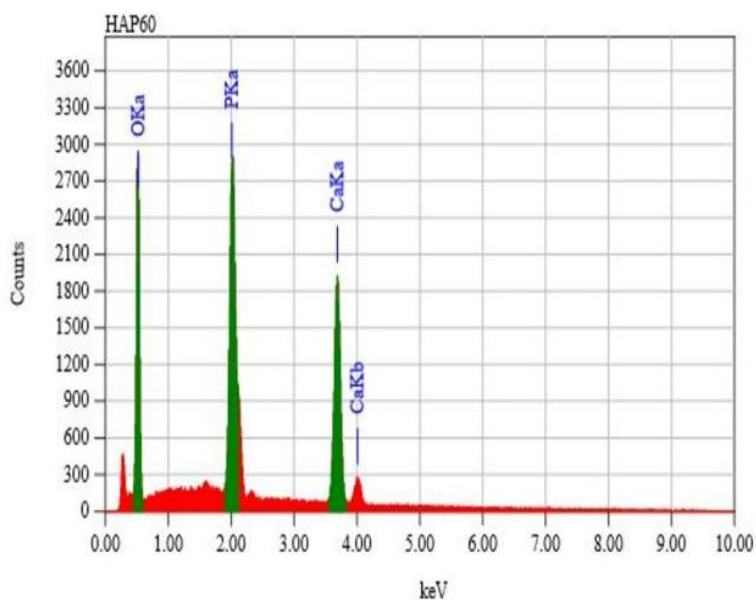


Figure 7. EDX analysis of synthesized HA with a stirring time of 60 min.

Table 2 Element composition of synthesized HA

Element	Mass (%)
O	40.74
P	19.15
Ca	40.11

3.5 Analysis of Thermal and Stability Properties

According to the DTA results shown in Figure 8, the enthalpy with the exothermic process for the HA with a stirring time of 60 min was 64.35 J/g. The HA with a stirring time of 60 min decreased in weight at 426.33°C, with a weight loss percentage of 0.834%. This weight loss was likely due to the evaporation of moisture water as a result of the CaO and (NH₄)₂ HPO₄ reactions. However, the HA with the stirring time of 60 min did not exhibit significant weight loss, making the graph profile tend toward the linear. This result indicates that the OH⁻ (crystal lattice) bond on the HA lattice did not break.

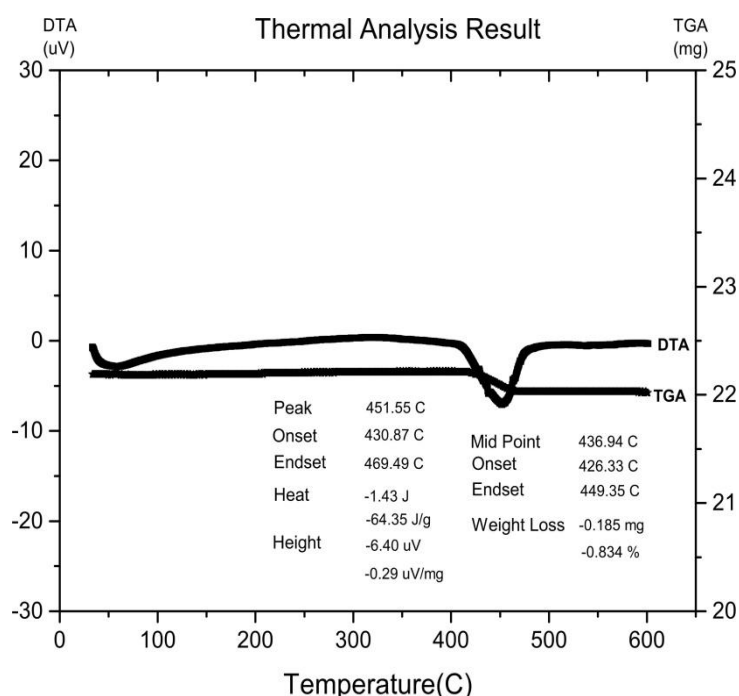


Figure 8. DTA/TGA for synthesized HA with a stirring time of 60 min.

Two types of water were observed in the HA: moisture (absorbed) and lattice (crystal) water. Moisture water was unstable between temperatures of 25-200°C, and loss of weight did not cause changes to the crystal lattice. The moisture water was a product of the reaction between the two precursors. The lattice (crystal) water was unstable between temperatures of 200 and 400°C, and severe weight loss caused contraction in the lattice dimensions during the heating process [28].

4. CONCLUSION

In this experiment, HA was synthesized successfully from green mussel shells through use of the precipitation method with variations of calcination temperature. The results of the AAS analysis showed that the Ca level at a calcination temperature of 950°C was 49.5757%. Per the XRD results, the calcium oxide calcined at 950°C exhibited the largest crystallite size, meaning it had high crystallinity and a shortened amorphous phase. The calcium oxide calcined at 950°C showed a small microstrain compared to the other samples, meaning the crystal defects in the sample were small. However, the crystallite size of the crystals was small when calcined at 850°C. Per the FTIR spectra result, the five samples all showed C-O functional groups of calcium carbonate contained in the green mussel shells. Non-calcined green mussel shells did not show the stretching mode of OH⁻ or the functional group of calcium oxide. The stretching mode of the OH⁻ groups started to form when calcination of the green mussel shells began at 650°C; however, the functional groups of calcium oxide started to form when calcination of the green mussel shells began at 750°C. Per the SEM results, the green mussel shells exhibited a large particle shape with a heterogeneous particle distribution. The green mussel shells calcined at 650°C were plate-like with a large and coarse particle shape. The green mussel shells calcined at 750°C showed a large and irregular particle shape. Some relief lines were visible on the surface of the particles after calcination at 850°C and 950°C. Per the DTA/TGA results, the green mussel shells calcined at 950°C experienced significant weight loss. This result indicates that large amounts of calcium carbonate content decomposed into calcium oxide at the temperature of calcination. The AAS, XRD, FTIR, DTA/TGA and SEM analyses helped determine that the calcium oxide sample calcined at 950°C should be used for HA synthesis with a stirring times of 60 min.

The crystallite size, microstrain, lattice parameter and x-ray density of the synthesized HA were (82.5±5.3) nm, 0.0061, 8.66Å and 10.27 g/cm³, respectively. These data demonstrate that the x-ray density value corresponded to the parameter lattice of the sample. According to the FTIR spectra, the sample had an HA functional group. According to the SEM images, the HA with the stirring time of 60 min had a small agglomerate shape and solid structure. The HA with a stirring time of 60 min also exhibited a Ca/P molar ratio of 1.67.

ACKNOWLEDGMENT

Monasari acknowledges the LPDP Scholarship, Indonesia (No. PRJ-62/LPDP/2016), and Yusril Yusuf acknowledges the Ministry of Research, Technology and Higher Education, Indonesia through the PUPT Grant (2456/UN1.P.III/DIT-LIT/LT/2017) for financial support in this research and payment of proofreading. The authors acknowledge the facilities and technical assistance from the staff at LPPT UGM, Indonesia.

REFERENCES

- [1] Indonesia. Ministry of Health RI, Center for Data and Information, *Data and Condition of Osteoporosis Disease in Indonesia*. Jakarta: Infodatin; 2015. [Online]. Available: <http://www.depkes.go.id/resources/download/pusdatin/infodatin/infodatin-osteoporosis.pdf>. [Accessed: Jan. 13, 2017].
- [2] N. Mulya, A. Fadli and A. Amri, "Effect on Addition of Hydroxyapatite to Stainless Steel 316L Metal Coating with Dip Coating Method," *Jom FTEKNIK*, **3**, 1 (2016) 1-7. [3]
- [3] S. Rujitanapanich, P. Kumpapan and P. Wanjanoi, "Synthesis of Hydroxyapatite from Oyster Shell via Precipitation," in *Proc. 11th Eco-Energy and Materials Science and Engineering (11th EMSES), 18-21 December 2013, Phuket, Thailand* [Online]. Belanda: Elsevier, 2014. Available: ScienceDirect, www.sciencedirect.com. [Accessed: 13 Jan. 2017].

- [4] M. Akram, R. Ahmed, I. Shakir, W. Ibrahim and R. Hussain, "Extracting Hydroxyapatite and its Precursors from Natural Resources," *J. Mater. Sci.*, **49** (2013) 1461-1475.
- [5] Y. Gao, W.-L. Cao, X.-Y. Wang, Y.-D. Gong, J.-M. Tian, N.-M. Zhao and X.-F. Zhang, "Characterization and Osteoblast-like Cell Compatibility of Porous Scaffold: Bovine Hydroxyapatite and Novel Hydroxyapatite Artificial Bone," *J. Mater. Sci. Mater. Med.*, **49** (2006) 815-823
- [6] F.-X. Huber, I. Berger, N. McArthur, C. Huber, H.-P. Kock, J. Hillmeier and P. Meeder, "Evaluation of Novel Nanocrystalline Hydroxyapatite Paste and a Solid Hydroxyapatite Ceramic for the Treatment of Critical Size Bone Defects (CSD) in Rabbits," *J. Mater. Sci. Mater. Med.*, **19** (2008) 33-38.
- [7] S. J. Kalita and S. Verma, "Nanocrystalline Hydroxyapatite Bioceramic Using Microwave Radiation: Synthesis and Characterization," *Mater. Sci. Eng. C*, **30** (2009) 295-303.
- [8] F. Mohandes, M. S.-Niasari, M. H. Fathi and Z. Fereshteh, "Hydroxyapatite Nanocrystals: Simple Preparation, Characterization and Formation Mechanism," *Mater. Sci. Eng. C*, **45** (2014) 29-36.
- [9] M. Saleha, N. Halik. Annisa, Sudirman and Subaer, Eds., *Proc. Scientific Meeting XXIX HFI Jateng & DIY, 25 April, 2015, Yogyakarta*. Yogyakarta: Proc. Scientific Meeting XXIX HFI, 2015.
- [10] H. Peng, J. Wang, S. Lv, J. Wen and J. F. Chen, "Synthesis and Characterization of Hydroxyapatite Nanoparticles Prepared by a High-Gravity Precipitation Method," *Ceram. Int.*, **41** (2015) 14340-14349.
- [11] S. C. Cox, P. Jamshidi, L. M. Grover and K. K. Mallick, "Low Temperature Aqueous Precipitation of Needle-Like Nanophase Hydroxyapatite," *J. Mater. Sci. Mater. Med.*, **25** (2014) 37-46.
- [12] R. Kumar, K. H. Prakash, K. Yennie, P. Cheang and K. A. Khor, "Synthesis and Characterization of Hydroxyapatite Nano-Rods/Whiskers," *Key. Eng. Mater.*, 284-286 (2005) 59-62.
- [13] F. Liu, F. Wang, T. Shimizu, K. Igarashi and L. Zhao, "Hydroxyapatite Formation on Oxide Films Containing Ca and P by Hydrothermal Treatment," *Ceram. Int.*, **32** (2006) 527-531.
- [14] S. -C. Wu, H. K. Tsou, H. C. Shu, S. -K. Hsu, S. P. Liu and W. -F. Ho, "Ceram. Int.", **39** (2013) 8183-8188.
- [15] S. -C. Wu, H. -C. Hsu, H. C. Shu, S. -K. Hsu, Y. -C. Chang and W. -F. Ho, "Synthesis of Hydroxyapatite from Eggshells Powders Through Ball Milling and Heat Treatment," *J. Asian Ceram. Soc.*, **4** (2015) 85-90.
- [16] M. Sari and Y. Yusuf, Eds., *Proc. The Biomaterials International, Aug. 20-24, Fukuoka, Japan, 2017*.
- [17] Muntamah, "Synthesis and Characterization of Hydroxyapatite from the Blood Mussel Shells (*Anadara granosa*, sp)," M.Si. Thesis, Institut Pertanian Bogor, Bogor, Indonesia, 2011.
- [18] A. Shavandi, A. E. -D. Bekhit, A. Ali, Z. Sun and J. T. Ratnayake, "Microwave-Assisted Synthesis of High Purity β - Tricalcium Phosphate Crystalline Powder from the Waste of Green Mussel Shells (*Perna canaliculus*)," *Powder. Tech.*, **273** (2014) 33-39.
- [19] W. Siriprom, N. Chumnanvej, A. Choeysuppaket and P. Limsuwan, "A Biomonitoring Study: Trace Metal Elements in *Perna viridis* Shell," *Proc. Eng.*, **32** (2012) 1123-1126.
- [20] G. Mc Mahon, *Analytical Instrumentation A Guide to Laboratory Portable and Miniaturized Instruments*. England: J. Willey and Sons Ltd, (2007) 130-170.
- [21] D. Zhang, S. Lu, L. L. Gong, C. -Y. Cao and H. -P. Zhang, "Effects of Calcium Carbonate on Thermal Characteristics, Reactions Kinetics and Combustion Behaviors of 5AT/Sr (NO₃)₂ Propellant," *Energy. Conv. Management.*, **109** (2015) 94-102.
- [22] A. Shavandi, A. E. -D. Bekhit, A. Ali and Z. Sun, "Synthesis of Nano-Hydroxyapatite (nHA) from Waste Mussel Shells Using a Rapid Microwave Method," *Mater. Chem. Phys.*, 149-150 (2015) 607-616.

- [23] M. Sari, "Synthesis and Characterization of Hydroxyapatite-Based on Green Mussel Shells (*Perna viridis*) with the Variation of Calcination Temperature and Stirring Time Using the Precipitation Method," M.Sc. Thesis, Universitas Gadjah Mada, Indonesia, 2017.
- [24] Kurnia, "Study on the Influence of Crystal Structure and Grain Size on Dielectric Properties of Manganese Ferrite ($MnFe_2O_4$) Nanoparticle," M.Sc. Thesis, Universitas Gadjah Mada, Yogyakarta, Indonesia, 2015.
- [25] J. H. Shariffuddin, M. I. Jones and D.A. Patterson, "Greener Photocatalysts: Hydroxyapatite Derived from Waste Mussel shells for the Photocatalytic Degradation of a Model Azo Dye Wastewater," *Chemic. Eng. Research. Design*, **91** (2013) 1693-1704.
- [26] D. Eichert, C. Drouet, H. Sfiha, C. Rey and C. Combes, *Nanocrystalline Apatite-Based Biomaterials*, New York: Nova Science Publishers, (2009) 15-20.
- [27] K. A. Gross, C. C. Berndt, P. Stephens and R. Dinnebier, "Oxyapatite in Hydroxyapatite Coatings," *J. Mater. Sci.*, **33** (1998) 3985-3991.
- [28] Suryadi, "Synthesis and Characterization of Hydroxyapatite Biomaterials by Wet Chemical Precipitation Process," MT. Thesis, Universitas Indonesia, Jakarta, Indonesia, 2011.

